ALFRED-WEGENER-INSTITUT
HELMHOLTZ-ZENTRUM FÜR POLAR- UND MEERESFORSCHUNG

725
2018

Berichte
zur Polar- und Meeresforschung

Reports on Polar and Marine Research

Russian-German Cooperation: Expeditions to Siberia in 2017

Edited by

Jens Strauss, Julia Boike, Dmitry Yu. Bolshiyanov, Mikhail N. Grigoriev, Hassan El-Hajj, Anne Morgenstern, Pier Paul Overduin and Annegret Udke
with contributions of the participants

HELMHOLTZ GEMEINSCHAFT

Die Berichte zur Polar- und Meeresforschung werden vom Alfred-Wegener-Institut, Helmholtz-Zentrum für Polar- und Meeresforschung (AWI) in Bremerhaven, Deutschland, in Fortsetzung der vormaligen Berichte zur Polarforschung herausgegeben. Sie erscheinen in unregelmäßiger Abfolge.

Die Berichte zur Polar- und Meeresforschung enthalten Darstellungen und Ergebnisse der vom AWI selbst oder mit seiner Unterstützung durchgeführten Forschungsarbeiten in den Polargebieten und in den Meeren.

Die Publikationen umfassen Expeditionsberichte der vom AWI betriebenen Schiffe, Flugzeuge und Stationen, Forschungsergebnisse (inkl. Dissertationen) des Instituts und des Archivs für deutsche Polarforschung, sowie Abstracts und Proceedings von nationalen und internationalen Tagungen und Workshops des AWI.

Die Beiträge geben nicht notwendigerweise die Auffassung des AWI wider.

Herausgeber
Dr. Horst Bornemann

Redaktionelle Bearbeitung und Layout
Birgit Reimann

Alfred-Wegener-Institut
Helmholtz-Zentrum für Polar- und Meeresforschung
Am Handelshafen 12
27570 Bremerhaven
Germany

www.awi.de
www.reports.awi.de

The Reports on Polar and Marine Research are issued by the Alfred Wegener Institute, Helmholtz Centre for Polar and Marine Research (AWI) in Bremerhaven, Germany, succeeding the former Reports on Polar Research. They are published at irregular intervals.

The Reports on Polar and Marine Research contain presentations and results of research activities in polar regions and in the seas either carried out by the AWI or with its support.

Publications comprise expedition reports of the ships, aircrafts, and stations operated by the AWI, research results (incl. dissertations) of the Institute and the Archiv für deutsche Polarforschung, as well as abstracts and proceedings of national and international conferences and workshops of the AWI.

The papers contained in the Reports do not necessarily reflect the opinion of the AWI.

Editor
Dr. Horst Bornemann

Editorial editing and layout
Birgit Reimann

Alfred-Wegener-Institut
Helmholtz-Zentrum für Polar- und Meeresforschung
Am Handelshafen 12
27570 Bremerhaven
Germany

www.awi.de
www.reports.awi.de

Titel: Das neu installierte klimatisierte Feldobservatorium-Iglu auf der Insel Samoylov, Lena Delta, beherbergt empfindliche Messgeräte, die an den meteorologischen Messturm im Hintergrund angeschlossen sind (Foto: Peter Schreiber, AWI).

Cover: The newly installed and climate-controlled observatory igloo on Samoylov Island, Lena Delta, houses sensitive measuring devices connected to the meteorological instrument tower in the background (Photo: Peter Schreiber, AWI).

Russian-German Cooperation: Expeditions to Siberia in 2017

Edited by

Jens Strauss, Julia Boike, Dmitry Yu. Bolshiyanov, Mikhail N. Grigoriev,

Hassan El-Hajj, Anne Morgenstern, Pier Paul Overduin and Annegret Udke

with contributions of the participants

Please cite or link this publication using the identifiers

http://hdl.handle.net/10013/epic.d436b7c2-6fb6-4543-813e-39e022d17bd5 and
https://doi.org/10.2312/BzPM_0725_2018

ISSN 1866-3192

Expeditions to Siberia in 2017

Research Station Samoylov Island and Lena Delta 02.04 - 26.09.2017

Drilling Campaign on Bykovsky Peninsula: Spring 2017 06.04 - 24.04.2017

Summer campaign on Bykovsky Peninsula 09.07 - 08.08.2017

Chief scientists

Julia Boike (AWI Potsdam), Dmitry Bolshiyanov (AARI), Svetlana Evgrafova (SIF), Alexey Fage (IPGG, NSU), Mikhail Grigoriev (MPI, IPGG), Guido Grosse (AWI Potsdam), Nikolay Mikhaltsov (IPGG, NSU), Anne Morgenstern (AWI Potsdam), Pier Paul Overduin (AWI Potsdam), Lasse Sander (AWI Sylt), Jens Strauss (AWI Potsdam)

Contents

4.1 Expedition Report – Bykovsky Peninsula Summer Expedition 2017

Michael Angelopoulos[1], Georgy Maximov[2], Bennet Juhls[3], Mikhail Grigoriev[2], Pier Paul Overduin[1], Aleksey Fage[4,5], Vladimir Olenchenko[4], Konstantin Sosnovtsev[5], Egor Esin[5], Polina Nikitich, [5,6], Andrey Kartozia[5], Vladimir Kashirtsev[4], Igor Yeltsov[4]

[1] Alfred Wegener Institute Helmholtz Centre for Polar and Marine Research, Potsdam, Germany

[2] Melnikov Permafrost Institute, Siberian Branch, Russian Academy of Sciences, Yakutsk, Russian Federation

[3] Institute of Space Sciences, Freie Universität Berlin, Berlin, Germany

[4] Trofimuk Institute of Petroleum Geology and Geophysics of Siberian Branch Russian Academy of Sciences, Novosibirsk, Russian Federation

[5] Novosibirsk State University, Novosibirsk, Russian Federation

[6] Institute of Soil Science and Agrochemistry, Siberian Branch, Russian Academy of Sciences, Novosibirsk, Russian Federation

[7] V.S. Sobolev Institute of Geology and Mineralogy of Siberian Branch, Russian Academy of Sciences, Novosibirsk, Russian Federation

Fieldwork period and location
July 09th to August 09th, 2017 (Bykovsky Peninsula)

Itinerary

Jul. 9: German participants travel to Tiksi

Jul. 11: Transfer to and establishment of basecamp at Uomullyakh-Kyuel Lagoon on the Bykovsky Peninsula

Aug. 1-6: Work aboard the Yacht Nicole in Tiksi Bay, Buor Khaya Bay and the Lena Delta

Aug. 5: Decamping from Uomullyakh-Kyuel Lagoon

Aug. 8: Travel from Tiksi to Yakutsk

Aug. 9: German participants return to Germany

Background and objectives
This expedition focused on interactions between water bodies and permafrost along the coast of the central Laptev Sea. This region is currently undergoing rapid environmental changes that include longer open water season, increasing snow depth, warming air and shelf sea temperatures, increasing river discharge, and freshening of shelf surface water. The consequences of these changes for the shelf ecosystem are likely to be severe, but it is not clear where the trajectory of change leads. Process studies and large-scale monitoring activities are necessary to understand the current state of the system and to be able to detect ongoing and future changes.
In April 2017, four sites were drilled on the Bykovsky Peninsula (Strauss et al., this volume). By connecting observations from the boreholes into geophysical surveys, the spatial distribution of permafrost beneath an incipient thermokarst lake, a thermokarst lake (Goltsovoye Lake), a saltwater lake within a drained freshwater lake basin (Polar Fox Lagoon), a coastal lagoon (Uomullyakh-Kyuel Lagoon) and in front of the coast can be analysed. Analysis of multi-temporal remote sensing data

provides a temporal context for the expansion of thermokarst water bodies, the progress of coastal erosion and sediment transport and the rates of permafrost aggradation and degradation.

Geophysical datasets, thermal modelling, and drilling data suggest that most Arctic shelves are underlain by submarine permafrost due to their exposure during the glacial low water stands (Romanovskii et al., 2004). The degradation of submarine permafrost could release large quantities of methane into the atmosphere, impact offshore drilling activities, and affect coastal erosion. The degradation of subsea permafrost itself depends on the duration of inundation, warming rate, the coupling of the seabed to the atmosphere from bottom-fast ice, and brine injections into the seabed (Overduin et al., 2012). The impact of brine injections on permafrost degradation is dependent on seawater salinity, which changes seasonally in response to salt rejection from sea ice formation and terrestrial freshwater inflows. The rate of submarine permafrost evolution and the relative importance of the many controls responsible for degradation, however, remain poorly understood. This work will evaluate submarine permafrost degradation rates on the Bykovsky Peninsula (north Siberia) using a combination of geophysical, sampling, and remote sensing methods. In addition, the work will study submarine permafrost thaw mechanisms and an approach to their representation using thermal modeling.
Sediment dynamics on the Siberian Shelf are changing but poorly constrained, especially coastal regions which are too shallow for research requiring larger marine vessels and year-round moorings. Nonetheless, the current dramatic reduction of sea ice thickness, extent and duration and rapidly changing land-to-ocean fluxes are impacting the ecosystem and oceanography of the shelf. The transition of the shelf ecosystem is due in particular to changing surface water dynamics, tied to ice thawing and freezing, river discharge, and the influx of nutrients, carbon, freshwater from coastal erosion. Monitoring and understanding the trajectory of these impacts requires remote sensing techniques. The observation of ocean colour with multi-spectral sensors permits estimation of changing shelf sediment dynamics and productivity. Furthermore, we target the unexplored but critical connection of submarine permafrost to sediment dynamics. Recent evidence, such as the disappearance of Ice Complex islands on the shelf (Romanovskii et al., 2004), the appearance of new shoals, and the migration of barriers and spits, suggest that sediment dynamics are changing, perhaps before we have a chance to establish an observational baseline for antecedent conditions. The use of ocean colour remote sensing data in arctic coastal waters is critical due to the optically complex properties (very turbid and cDOM rich waters) and the size and remoteness of the study area. The paucity of data from the region makes simultaneous measurement of optical properties and surface water chemistry necessary for the interpretation and application of ocean colour data.
Our objectives are to i) measure the distribution of permafrost-relevant geophysical parameters beneath water bodies representing various stages in the transition of terrestrial to submarine permafrost, which will allow us to quantify rates of permafrost degradation and ii) measure and apply above-water and water column radiometric measurements for the evaluation of satellite ocean colour products. The latter, combined with analyses of surface water for its constituents, will help us to understand how the optical properties of different water masses are tied to processes integral to shelf ecosystem and oceanography. *In situ* concentrations of different biogeochemical water constituents alongside with above-water and in-water reflectance measurements will be used within radiative transfer simulations to improve a better retrieval of the optical water properties via remote sensing data.

Site description

The Bykovsky Peninsula is located east of the Lena Delta in the western part of the Buor-Khaya Gulf of the Laptev Sea in northeastern Siberia, Russia (Figure 4.1-1). Cape Moustakh, the southeastern limit of the peninsula, is located approx. 20 km east-northeast of Tiksi, a harbour town and the closest urban settlement. The peninsula is an erosional remnant of an accumulation plain on the foreland of the Kharaulakh Ridge that started to form in the Late Pleistocene. The erosion of the Kharaulakh Ridge through nival and seasonal hydrological processes was the main sediment supply for the accumulation of medium to fine-grained ice-rich deposits known as the Yedoma Ice Complex. During the late stage of the Weichselian glaciation, increased meltwater resulted in higher erosion rates of the Kharaulakh Ridge's valley deposits, which ultimately disconnected the accumulation plain from its sediment source. In the early Holocene, a warming climate resulted in intense thermokarst development. Following deglaciation, marine transgression and ingression, as well as mechanical and thermal erosional processes, produced the landscape of the Bykovsky Peninsula seen today. The Yedoma Ice Complex can extend from the top of the peninsula's highlands (up to 45 m above sea level) to 10 m below sea level. However, the base of the Yedoma Ice Complex can be as high as 1 m below sea level in the Western Bykovsky Peninsula and 10 m below sea level in the Eastern Bykovsky Peninsula. Moustakh Island, also an erosional remnant, is located 15 km southeast of the Bykovsky Peninsula and also shows that the Yedoma Ice Complex can reach 10 m below sea level. Furthermore, the total ice content (wedge ice and intrasedimentary ice) can be up to 87 % by volume. Sediments within the Yedoma Ice Complex at or below sea level on the Bykovsky Peninsula mainly range from silt to fine sand. The depth to coarse-grained sandy gravel was reported to be as high as 9 m below sea level on the Western Bykovsky Peninsula and up to 29 m below sea level on the Eastern Bykovsky Peninsula. In between the Yedoma Ice Complex and the coarse-grained deposits, the soil type ranges from silty sand to sand and may contain massive cryostructures. Offshore of the Bykovsky Peninsula, part of the Yedoma Ice Complex is submerged and subsea permafrost is currently degrading. The thickness of subsea permafrost on the Laptev Sea shelf can be hundreds of metres thick and its presence can possibly extend up to 350 km offshore. Offshore of Moustakh Island, repeated borehole measurements separated by 31 - 32 years show an ice-bearing subsea permafrost degradation rate of 0.14 m per year. Furthermore, geoelectric observations offshore of Moustakh Island show that the degradation rate of ice-bearing subsea permafrost decreased from 0.4 m per year after inundation to 0.1 m per year 60 - 110 years after submergence. They also demonstrated that the depth to ice-bearing subsea permafrost at a given distance perpendicular to shore is inversely correlated with the coastal erosion rate. On the Bykovsky Peninsula, the coastal erosion rate is related to the orientation of the shoreline. From 1951-2006, the mean erosion rate was as high as 1.05 m per year for north-facing shores and as low as 0.42 and 0.27 m per year for south-facing and southeast-facing shorelines, respectively. The southern shoreline of the Bykovsky Peninsula lies in Tiksi Bay, which is a marine environment affected by the outflow of the Lena River. Due to its isolation behind Moustakh Island and Cape Moustakh, sea ice tends to be preserved longer than in the Central Laptev Sea. Northeast of Muostakh Island in 7.2 m water depth, recorded hourly benthic temperature and electrical conductivity data from 01.09.2008 to 31.08.2009. The mean annual seabed temperature was 0.5 °C, but seabed temperatures reached values lower than -1 °C below the ice in winter and spring. The mean annual electrical conductivity of the water was 7.1 mS/cm, but values can be as high as 35 mS/cm underneath the ice in winter. Following ice break-up, the influence of the Lena River discharge results in an electrical conductivity less than 0.3 mS/cm. The sea ice season in Tiksi Bay and the Buor-Khaya Gulf typically starts in late September/early October and ends in June. The mean annual air temperature in Tiksi between 1932 and 2016 was -12.8 °C (World Meteorological Organization station in Tiksi) and the average day for which air temperatures started to dip below 0 °C was September 25^{th}.

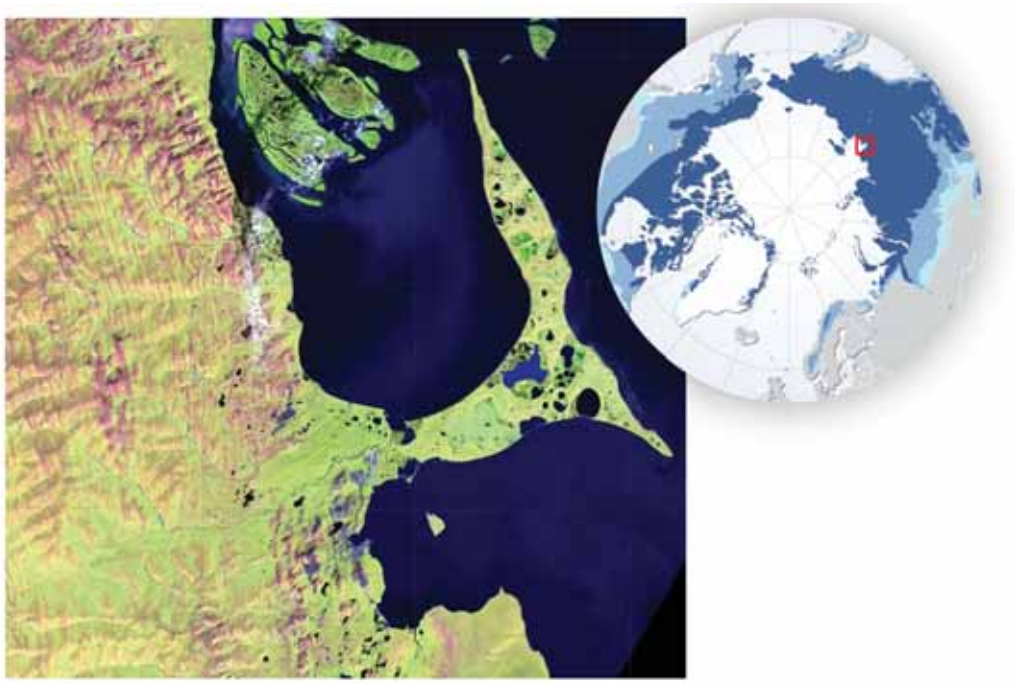

Figure 4.1-1: *Location of Bykovsky Peninsula*

Methods

Meteorological observations

A Davis Vantage Vue wireless weather station was employed at the Uomullyakh-Kyuel Lagoon to measure camp air temperature, precipitation, relative humidity, barometric pressure, wind speed and wind direction. The station was installed on a hilltop behind the camp, at location 71.73592 N, 129.29983 E. The data were recorded hourly for the period from 13.07.2017 10:00 to 04.08.2017 20:00.

- The instrument was mounted 1.7 m above the ground surface on a tripod at an elevation of 7.7 m above sea level. The tripod was secured in place with three ropes tied to tent pegs in the ground (Figure 4.1-2).
- The elevation value was extracted from a 2015 one-meter resolution digital elevation model. This value was passed to the Vantage Vue console to calibrate the barometric pressure reading.
- The instrument's wind speed detection limit was 0.83 m/s (3 km/hour).
- The instrument's rain collector measured precipitation in 0.2 mm increments.

Figure 4.1-2: *The Davis Vantage Vue meteorological station setup at Uomullyakh-Kyuel Lagoon camp on 2017-07-23*

Active layer survey

Three north to south active layer surveys were carried out, each traversing Yedoma upland permafrost, a beach terrace, and the floodplain (Figure 4.1-6). In general, the deepest active layers were recorded on the terrace. More specifically, the average active layer thickness values were 0.43, 0.54, and 0.44 m for the upland permafrost, beach terrace, and floodplain respectively. The deepest active layer thickness (0.88 m) was measured on the terrace of Profile 2 on July 18th, 2017 (Figure 4.1-4). The thinnest active layer (0.23 m) was measured on the upland of Profile 1 on July 13th, 2017. (Figure 4.1-3). The deeper active layers on the terrace are likely due to the absence of a dense insulating vegetation layer, as well as separation from the occasionally submerged tidal floodplain. Hence, the scarcely vegetated terrace likely has the greatest exposure to warm summer air temperatures.

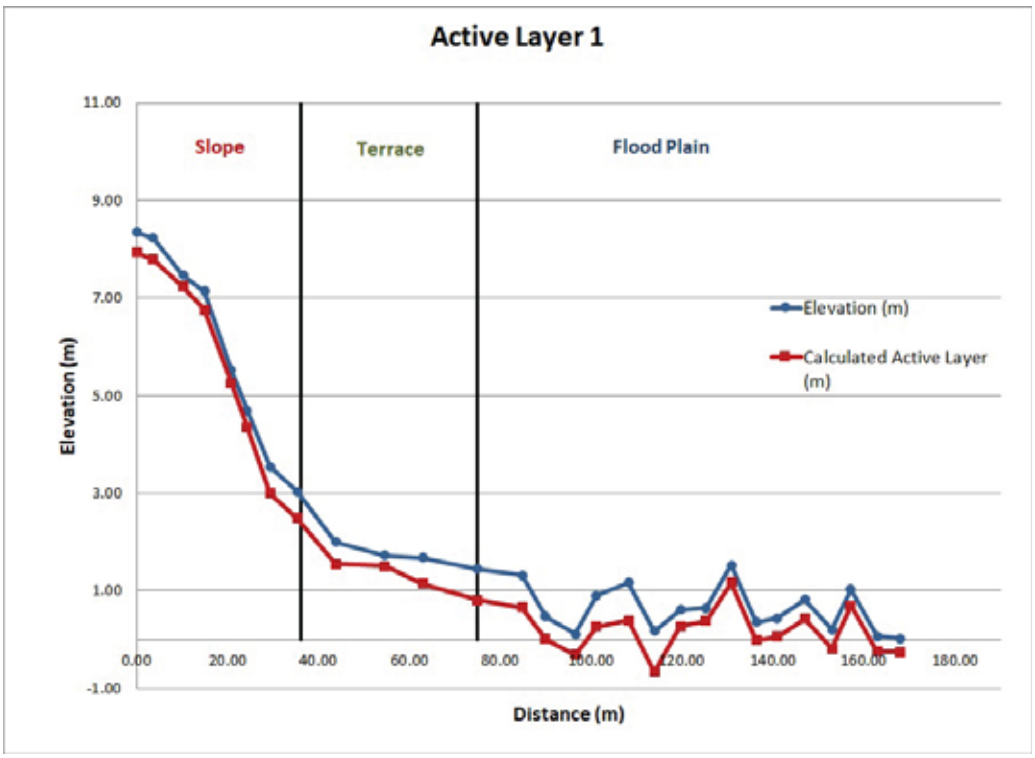

Figure 4.1-3: *North to South active layer survey in order to find out depth and thickness. Results for active layer 1*

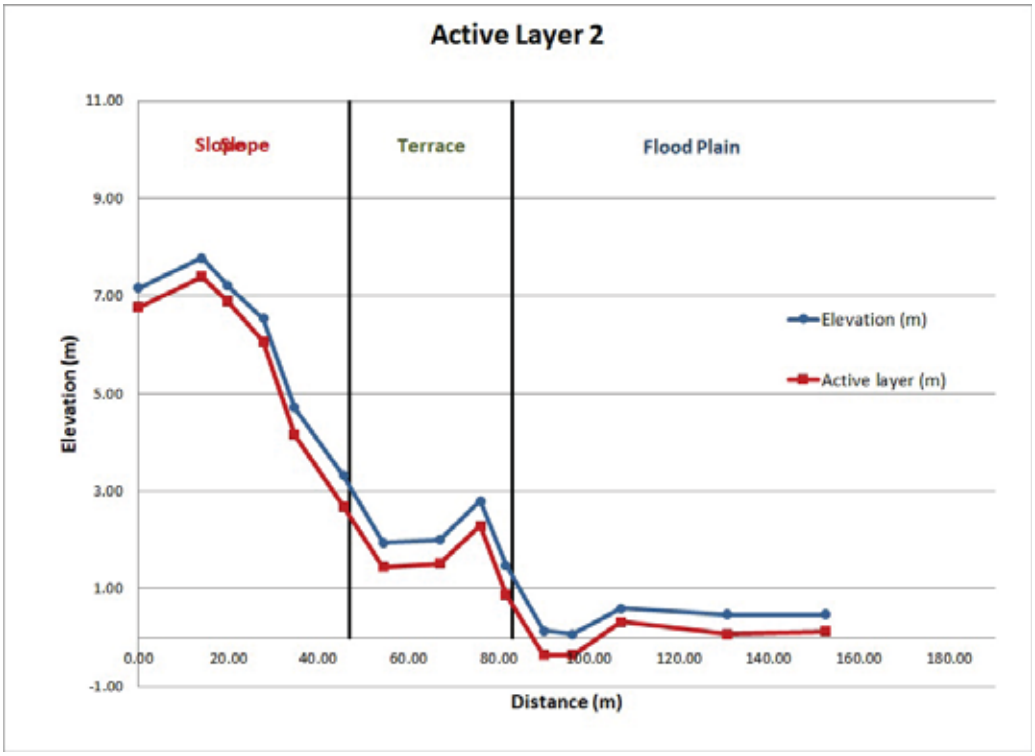

Figure 4.1-4: *North to South active layer survey in order to find out depth and thickness. Results for active layer 2*

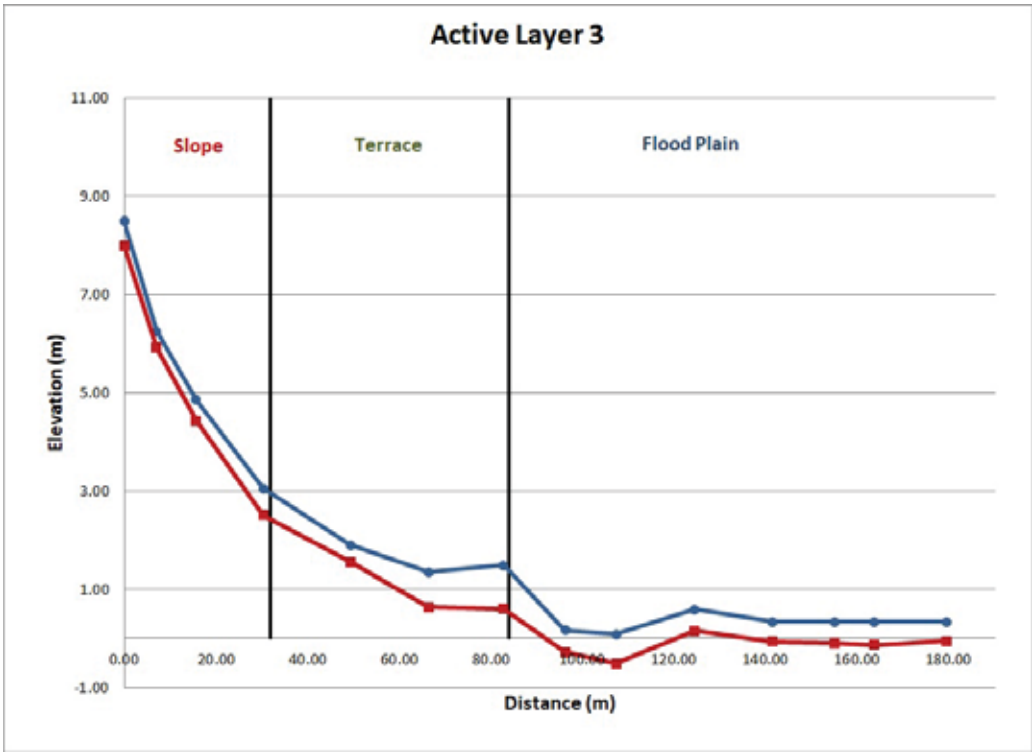

Figure 4.1-5: *North to South active layer survey in order to find out depth and thickness. Results for active layer 3*

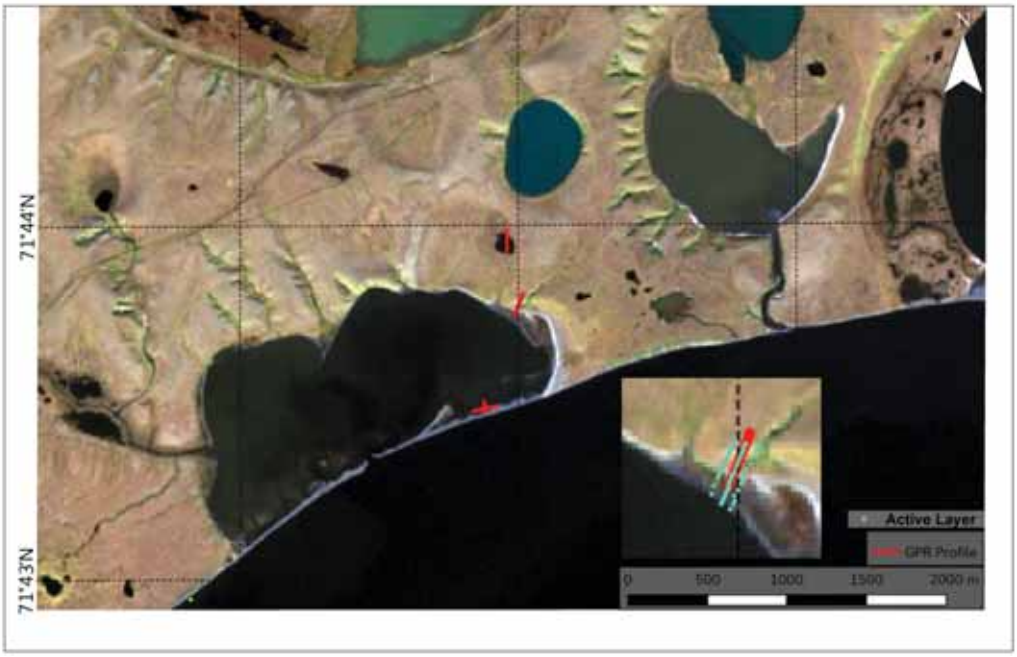

Figure 4.1-6: *Active Layer Map*

Electrical resistivity

The main goal of electrical resistivity tomography (ERT) surveying was to map unfrozen and frozen sub-aquatic sediments at Goltsovoye Lake, Polar Fox Lagoon, Uomullyakh-Kyuel Lagoon, and the nearshore coastal zone just offshore of Uomullyakh-Kyuel Lagoon. Terrestrial permafrost surveys were performed at Uomullyakh-Kyuel and Polar Fox Lagoons to relate thawing sub-aquatic

permafrost with undisturbed terrestrial permafrost. Offshore work also included surveys of the Lena River Delta Channel. The ERT method is effective at delineating unfrozen and frozen sediment, because there is an increase in electrical resistivity as water freezes to form ice (e.g. Kneisel et al., 2008). However, this increase in resistivity is mainly due to the decrease in unfrozen water content. Therefore, the resistivity of sub-aquatic permafrost soils is highly dependent on porosity, grain size, temperature, and the quantity of total dissolved solids in the porewater, all of which affect unfrozen water content. As a result, the transition from relatively low to high resistivity could be sharp or gradual depending on the nature of sub-aquatic conditions and stratigraphy. In addition, the order of magnitude for what constitutes a frozen sub-aquatic soil in terms of electrical resistivity is site-specific.

Not including surveys offshore of the Bykovsky Peninsula, three sites characterized by unique boundary conditions in early spring were investigated: 1) a deep freshwater lake with no ice grounding in the centre of the lake (Goltsovoye Lake), 2) a saltwater lake with no ice grounding in the centre of the lake (Polar Fox Lagoon), and 3) a shallow saltwater lagoon with ubiquitous ice grounding (Uomullyakh-Kyuel Lagoon). The boundary conditions are summarized in Figure 4.1-9. Due to the saltwater at Polar Fox Lagoon, the near-surface sediments below the lakebed were also suspected to be salty. In October 2017, the German Research Centre for Geosciences (GFZ) performed porewater chemistry analyses of samples collected by the UWITEC^{TM} coring team during the April 2017 expedition. In the uppermost metre of sediment, the maximum electrical conductivity of the porewater was 52,300 μS/cm, which translates to a freezing point of approx. –2.2 °C. At Uomullyakh-Kyuel Lagoon, grounded ice conditions were encountered at all ice auger locations in April 2017 and therefore the salt concentrations in the sediment are suspected to be even higher compared to Polar Fox Lagoon.

At the saltwater sites, an IRIS Syscal Pro Deep Marine (ISPDM) system was used for all resistivity surveys. For freshwater lakes and channels, as well as terrestrial permafrost settings, the standard IRIS Syscal Pro (ISP) system was used. The ISPDM produces a higher maximum current output (50 amperes) compared to the ISP, which produces a maximum current output of 2.5 amperes. However, the ISPDM has a lower transmitter output voltage (200 volts) compared to the ISP (2000 volts). In very conductive environments like saltwater lagoons, the ISPDM is well-suited to produce the high current intensity forced by the low resistivity water layer in contact with the electrodes, whereas in more resistive environments like freshwater lakes and terrestrial permafrost, a higher transmitter voltage is needed to generate sufficient current intensity.

For all surveys on water, a 120 m or 60 m geoelectric cable with floating electrodes was towed behind a small inflatable boat with a 5 horse-power outboard motor (Figure 4.1-10). Both the ISPDM and ISP were equipped with a GPS and an echo sounder to record the position and water depth at the boat locations. The 120 m and 60 m cables had electrode separations of 10 m and 5 m, respectively. In total, two current electrodes and 11 potential electrodes were used. Both the ISPDM and the ISP have 10 channels and can thus measure 10 voltages with different combinations of the current electrodes and two potential electrodes simultaneously. The only array type used for the sub-aquatic surveys was the Reciprocal Wenner-Schlumberger array as shown in Figure 4.1-11(a). For nearly all water surveys, measurements were taken every 5 m of trip distance. However, in areas with rapidly changing bathymetry like the baydjarakh structures beneath Goltsovoye Lake, a 1 m measurement interval was occasionally used. An overview of geoelectric surveys is presented in Figure 4.1-7 for Uomullyakh-Kyuel Lagoon, Polar Fox Lagoon, and Goltsovoye Lake, as well as in Figure 4.1-8 for the Byskovskaya outflow channel of the Lena Delta. A detailed summary of profile settings and start/end coordinates are shown in Table A.4-1 for water surveys and Table A.4-2 for terrestrial surveys.

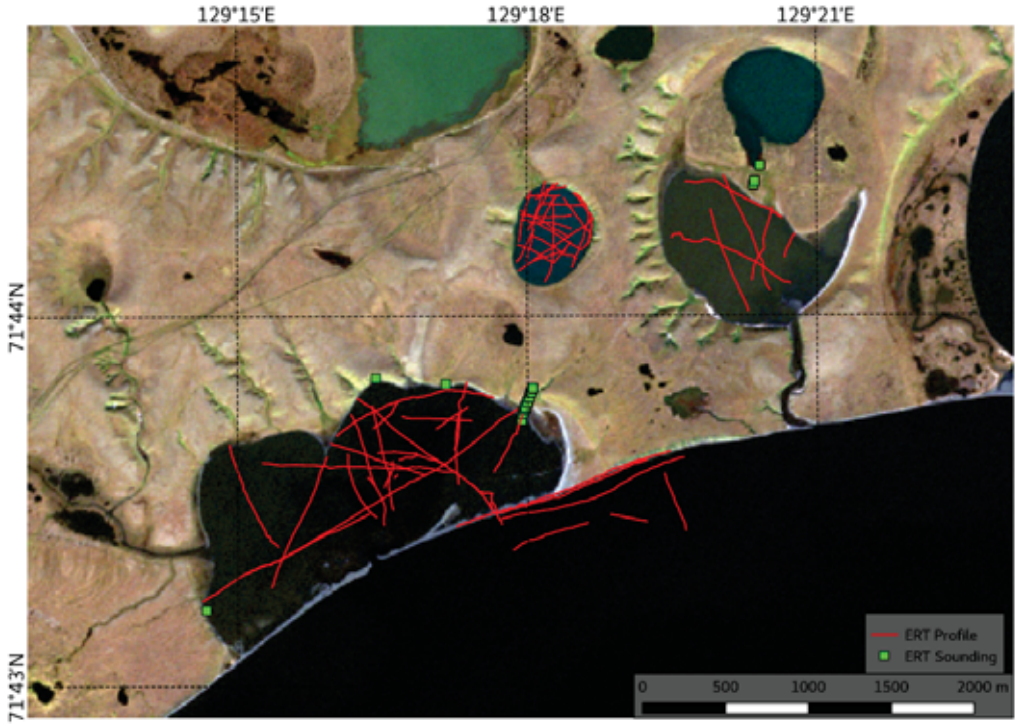

Figure 4.1-7: *ERT Soundings and Profiles in Uomollyakh-Kyuel Lagoon*

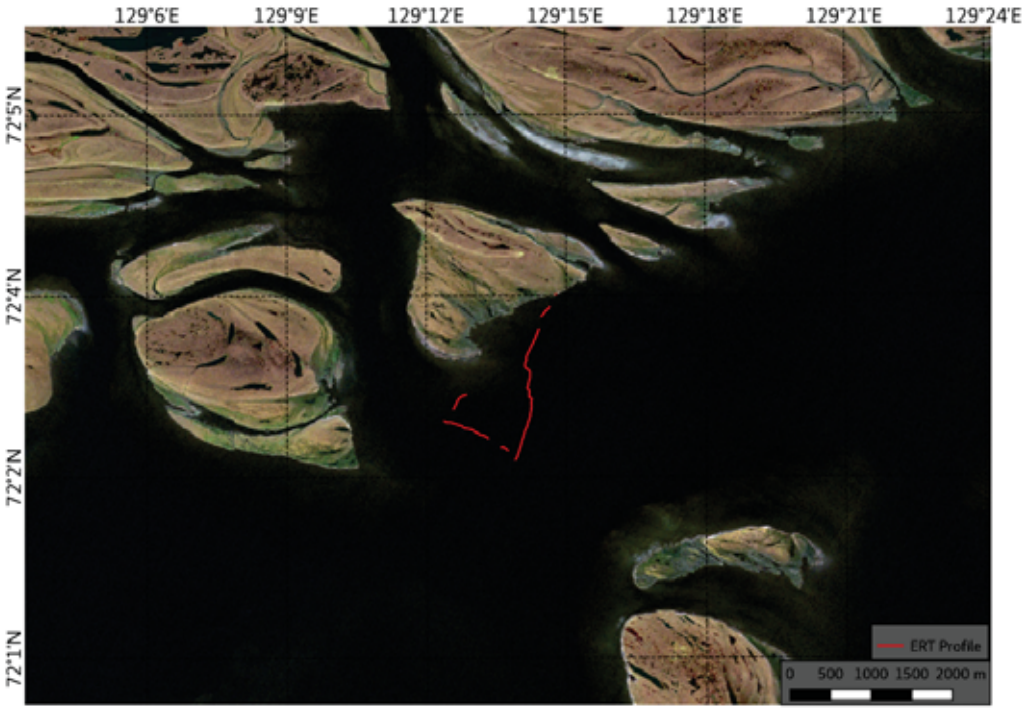

Figure 4.1-8: *ERT Profiles in the Bykovskaya outflow channel*

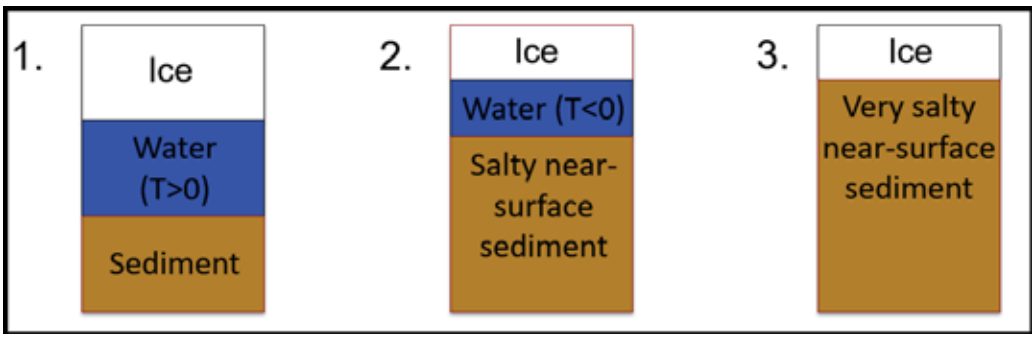

Figure 4.1-9: *Boundary conditions at borehole locations in April 2017 at Goltsovoye Lake (1), Polar Fox Lagoon (2), and Uomullyakh-Kyuel Lagoon (3) and the suspected sediment characteristics*

Water surveys

Uomullyakh-Kyuel Lagoon and Offshore

In total, 37 surveys were collected in Uomullyakh-Kyuel Lagoon and offshore of the lagoon in the nearshore coastal zone with a 10 m electrode spacing to maximize penetration depth. In addition, 6 surveys were taken in the freshwater Bykovskyaya channel of the Lena Delta. The first priority in Uomullyakh-Kyuel Lagoon was to collect west to east, as well as north to south profiles intersecting the deep borehole location from the April 2017 expedition. The temperature and stratigraphic information available from the borehole is critical for geophysical interpretation. The second priority was to collect resistivity data across the west to east, as well as the two north to south transient electromagnetic survey lines carried out by the Institute of Petroleum Geology and Geophysics (IPGG) in April 2017. The IPGG profiles were taken along the same lines as the ground-penetrating radar surveys performed by Timer LLC (Figure 3.5-6). The next goal was to collect a series of ERT profiles perpendicular to Uomullyakh-Kyuel Lagoon and offshore shorelines characteristic of both Alas and Yedoma permafrost terrain. The rationale for these surveys is to plot the position of the ice-bearing permafrost table with the ERT as a function of distance away from the shoreline. When tied in with shoreline erosion rates inferred from historical remote sensing imagery, an ice-rich permafrost degradation rate can be calculated. Of particular interest is investigating how the ice-rich permafrost table slopes differ between Alas and Yedoma permafrost. Having already undergone a thermokarst and refreezing cycle, it is speculated that the Alas terrain could have less ice content and a warmer initial ground thermal regime upon inundation compared to the Yedoma. Hence, the ice-rich permafrost table degradation rate is potentially faster for eroding Alas shorelines. Perhaps even more curious were the surveys crossing the lagoon's southern sand bar adjacent to the sea. The results to date suggest permafrost is aggrading beneath the center of the sand bar, but since the spit is a very dynamic feature, this newly formed permafrost will soon be inundated with seawater as the spit retreats further north. Therefore, it is also speculated that a "permafrost tail" exists south of the spit where recently formed permafrost (i.e. decadal time-scale) is currently degrading due to inundation. In an effort to map near-surface frozen soils below and south of the spit, higher resolution surveys with a 5 m electrode spacing were carried out in the addition to the standard 10 m electrode spacing. Critical to all the aforementioned science questions is knowing the resistivity signatures of undisturbed permafrost, as well as inundated permafrost right at the shoreline. Knowing full well the pitfalls of three-dimensional geology and how they pertain to electrical current propagation, three one-dimensional soundings with the 120 m cable parallel to the shoreline were taken along Uomullyakh-Kyuel Lagoon's western and northern shorelines. Furthermore, considerable effort was invested to acquiring a water survey that overlaps the terrestrial active layer and resistivity transects described in Section *Terrestrial Survery, Uomullyakh-Kyuel Lagoon*.

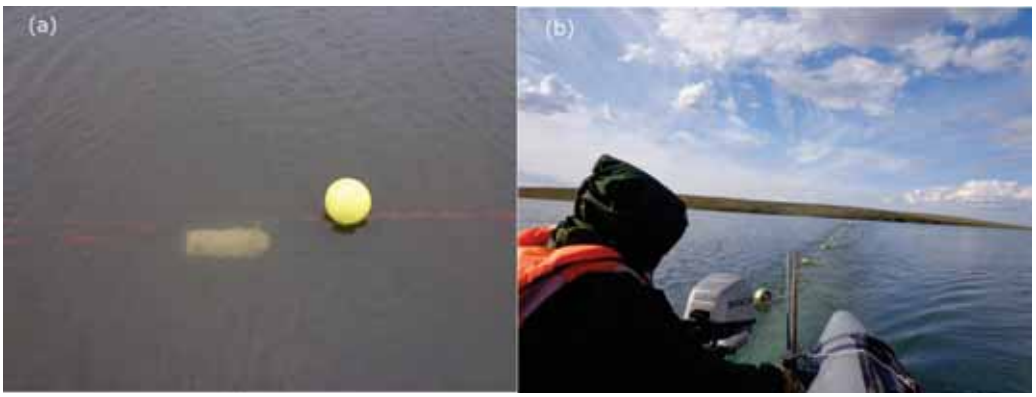

Figure 4.1-10: *(a) For water surveys, thin metal plates were used as electrodes and hung approx. 10 cm below the top of the water surface by attaching buoys to the cable. (b) The geoelectric cables were towed behind a small inflatable motor boat.*

Polar Fox Lagoon

In total, 6 surveys were collected at Polar Fox Lagoon with a 10 m electrode spacing to maximize penetration depth. Similar to Uomullyakh-Kyuel Lagoon, the first priority was to collect west to east, as well as north to south profiles intersecting the deep borehole and UWITEC^{TM} coring locations from the April 2017 expedition. The second objective was to intersect the April 2017 one-dimensional ERT sounding location. This is exciting, because the seasonal comparison could show transient resistivity changes in the near-surface due to warming sub-aquatic soil temperatures from April to July. Since the temperature chain data exists only for April 2017, the multi-season ERT data could shed light on the depth of zero annual amplitude. The latter is particularly important to grasp at Polar Fox Lagoon, because the soil temperatures were very close to 0 °C at all depths in April 2017. Thus, small seasonal changes in temperature could have profound impacts on unfrozen water content, as well as the frozen/unfrozen state of the soil. To acquire an electrical resistivity signature of the permafrost just above the shoreline, a mixed terrestrial and floating electrode survey was carried out. More specifically, the centre of the Reciprocal-Schlumberger array was placed at the shoreline, such that 7 floating electrodes were placed in the water, and 6 electrode nails were inserted into the tundra. Once a measurement was taken, the boat moved 10 m further offshore as the entire array was moved 10 m towards the lake. This process continued until all floating electrodes were in the water. At this point, the measurements continued as a water survey with resistivity values recorded every 5 m of trip distance.

Goltsovoye Lake

At Goltsovoye Lake, 23 surveys were carried out. The 5 m electrode spacing was used for all surveys because: 1) Due to the lake's relatively small size, greater mobility with the motor boat and the cable was desired, 2) High resolution data below baydjarakh structures was optimal to identify potentially submerged ice wedges, and 3) The talik thickness at the April 2017 deep borehole location was already known (31 m below the top of the water surface) and thought to be beyond the maximum depth of investigation for surveys with a 10 m electrode spacing. Note that the 60 m cable used for these surveys has fixed positions for the current electrodes and thus the Reciprocal Schlumberger Array configuration (Figure 4.1-11(b)) was slightly different than Uomullyakh-Kyuel Lagoon and Polar Fox Lagoon. In addition to intersecting the deep borehole and UWITEC^{TM} drilling locations from April 2017, one of the science goals was to conduct ERT surveys over the methane bubble photo lines from the spring expedition. The photo profile showed bubbles trapped in the lake ice, which were interpreted as methane gas emissions from thawing sub-aquatic permafrost. Although no terrestrial surveys were performed at Goltsovoye Lake, the IPGG performed extensive land surveys over Yedoma and Alas permafrost in between Uomullyakh-Kyuel Lagoon and Goltsovoye Lake with a 5 m electrode spacing.

Terrestrial surveys

Uomullyakh-Kyuel Lagoon

For terrestrial surveys at Uomullyakh-Kyuel Lagoon, a total of 64 one-dimensional soundings were carried out at 12 locations along an active layer monitoring transect (refer to Section *Active Layer Survey*) with an electrode spacing of 5 m and the ISP. The active layer profile started in the lagoon's shallow northern waters close to camp and progressed further north perpendicular to shore for a total length of 170 m. The profile crossed an occasionally inundated zone with scarce vegetation, a small bluff, and undisturbed upland permafrost tundra. At 9/12 sounding locations, surveys were taken with the geoelectric cable oriented perpendicular to Uomullyakh-Kyuel Lagoon's shoreline and thus parallel with the active layer transect. At 6/12 sounding locations, surveys were taken with the geoelectric cable oriented parallel to Uomullyakh-Kyuel Lagoon's shoreline and thus perpendicular to the active layer transect. While the orientation of the cable affects the half-space and thus the resistivity of the subsurface medium in which the electrical current propagates, the surface position below which the apparent resistivity depth points are located, remains the same. At the sounding locations, the surveys included variations in receiver voltage range (5 volts and 15 volts) and the array type. The arrays used were Reciprocal Wenner Schlumberger (Figure 4.1-11(a)), Wenner Schlumberger (Figure 4.1-11(c)), Dipole-Dipole-A (Figure 4.1-11(d)), and Dipole-Dipole-B (Figure 4.1-11(e)). The active layer transect was also surveyed by the IPGG using a 2.5 m electrode spacing and a Wenner Schlumberger array configuration.

Polar Fox Lagoon

For terrestrial surveys at Polar Fox Lagoon, a total of 13 one-dimensional soundings were carried out at 3 locations on a land bridge separating salty Polar Fox Lagoon and a smaller freshwater lake to the north. Since both water bodies exist within the same basin, the land bridge was likely flooded in the past. Furthermore, remote sensing imagery dating back to 1951 shows that the land bridge has been drying up and/or growing in extent over the past several decades. Therefore, the goal of this investigation was to determine if the land bridge overlies a currently re-freezing talik. The surveys were carried out with the ISP, a 10 m electrode spacing, 5 volt and 15 volt receiver voltages, as well as both Reciprocal Wenner Schlumberger and Wenner Schlumberger arrays.

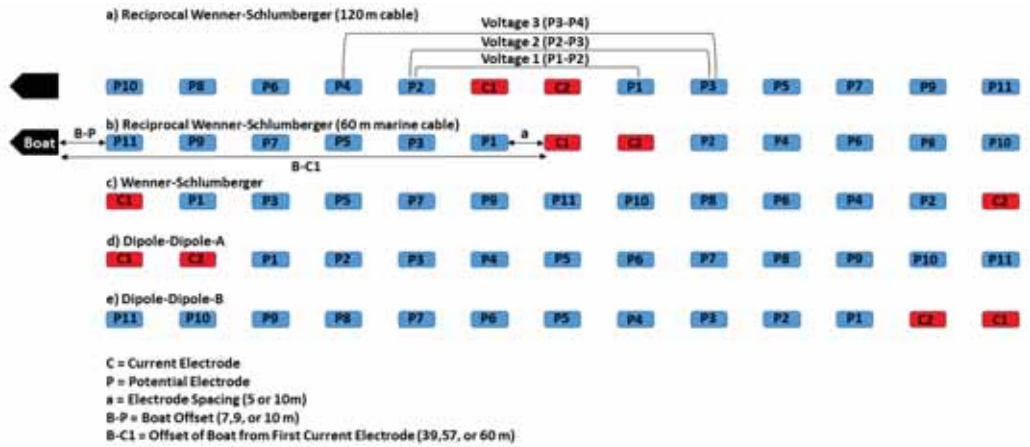

Figure 4.1-11: *The different array configurations used included the Reciprocal Schlumberger configuration for the 120 m cable (a), the Reciprocal Schlumberger configuration for the 60 m marine cable (b), the Wenner Schlumberger array (c), the Dipole-Dipole-A setup (d), and the Dipole-Dipole-B configuration (e). For each array type, 10 voltages were recorded simultaneously for each measurement point using the current electrodes and a pair of potential electrodes. The potential electrode pairs follow the P1-P2,P2-P3,P3-P4,P4-P5,P5-P6,P6-P7,P7-P8,P8-P9,P9-P10, and P10-P11 sequence for all array types.*

Ground-penetrating radar

Ground-penetrating radar (GPR) transmits electromagnetic waves (approx. 10 to 1000 MHz) into the subsurface and records reflections at boundaries between materials with different dielectric constants. Since the dielectric constant of a soil sharply decreases as water freezes to form ice, GPR has proven to be effective at mapping unfrozen/frozen soil interfaces, as well as ground ice bodies (e.g. Angelopoulos et al., 2013; Moorman et al., 2003). GPR surveys were performed at a small alas lake in between Goltsovoye Lake and Uomullyakh-Kyuel Lagoon, Uomullyakh-Kyuel Lagoon's sand bar, as well as the active layer transect described in *Section Active Layer Survey*. To maximize the possibility of detecting deep unfrozen/frozen soil boundaries, the 50 MHz MALA Geoscience rough terrain antenna was used for all surveys. Since saltwater severely attenuates GPR signals (e.g. Annan, 2004), no surveys were carried out in the waters of Uomullyakh-Kyuel and Polar Fox Lagoons. The small Alas lake was a site of particular interest during the spring expedition to its small size, proximity to camp, and promising initial GPR results. 50 MHz profiles from the spring showed structures below the lake-bottom reflector, but it was unclear whether the structures were real or artefacts generated by a combination of side reflections from the lake edges and multiple reflections from the ice/water and water/sediment interfaces. Therefore, the south to north profile line was repeated in summer by towing the antenna behind a small inflatable kayak (Figure 4.1-13). The antenna was wrapped in thin plastic film to keep it dry and six empty water bottles were attached to the antenna to make it float. The rationale for investigating Uomullyakh-Kyuel Lagoon's sand bar with the GPR was to map the underlying frozen soil bulb geometry that the authors suspect is forming due to permafrost aggradation. Even with 50 MHz, the vertical resolution of GPR is superior to ERT surveys with a 5 m electrode spacing. To maximize resolution in the near-surface, 200 MHz GPR surveys were attempted, but they failed due to equipment problems. In total, 2 north-south and 2 west-east profiles were taken in both possible directions at the ERT transect location. Lastly, south to north, as well as north to south GPR profiles were carried out along the active layer transect. In this scenario, the exploration of penetration depth as a function of distance away from the shoreline was of particular interest. Since electrically conductive saltwater attenuates GPR signals, changes in penetration depth across the survey line could detect lateral transitions of salty sediment, particularly below the occasionally submerged sandy beach. An overview of GPR surveys is presented in Figure 4.1-12 and a detailed summary of profile settings and start/end coordinates are shown in Table A.4-3.

Figure 4.1-12: *GPR Profiles*

Figure 4.1-13: *Floating 50 MHz ground-penetrating radar survey at a small alas lake between Goltsovoye Lake and Uomullyakh-Kyuel Lagoon*

Radiometry

Radiometric measurements included above-water and in-water measurements with different instruments (discussed below). For a better orientation of light and sky conditions during the measurements, photos of the sky and the water were taken according to the view angles of the

measurements. All measurements were carried out with an anchored boat to avoid strong drift. The duration of all measurements at one station took between 30 and 60 minutes. Only at good light conditions (clear sky) radiometric measurements were carried out. However, sky conditions changed for some stations during the period of measurement. These changing conditions have to be filtered during the data analysis.

Above-water

Above-water radiometric measurements were taken at selected stations using a handheld 3-radiometer (Hamamatsu). The radiometer provides high resolution hyperspectral measurements of the downwelling irradiance (Ed), downwelling radiance (Lsky) and the total upwelling radiance (Lu) (Figure. 4.1-14).

An absolute radiometric calibration was done for each radiometer before the expedition using a spectralon plate and a FEL lamp as a spectral irradiance reference standard. For each measurement the dark current of the radiometers were measured which will be subtracted from the measured intensities. Intercalibration of all 3 sensors were done taking a grey spectralon plate for both radiance sensors.

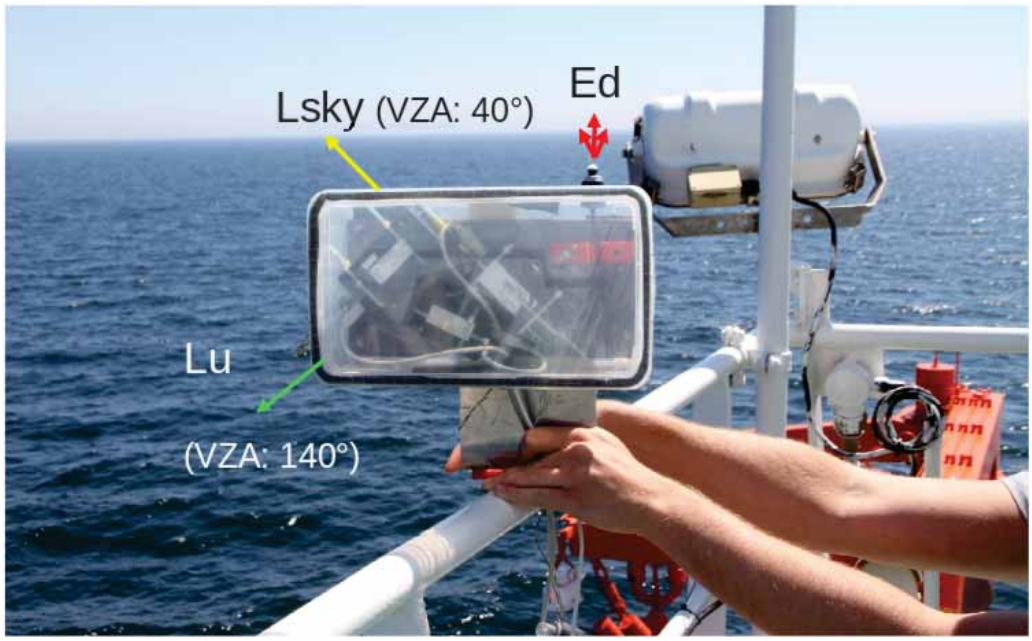

Figure 4.1-14: *Handheld 3-Radiometer with 2 radiance and 1 irradiance spectroradiometers*

In-water

In addition to above-water radiometric measurements, in-water radiometric measurements were taken at the same stations with two TRIOS Ramses irradiance sensors (Figure. 4.1-15). The in-water downwelling and upwelling irradiance (Ed and Eu) was measured at different depths depending on the transparency of the water. In-water measurements will provide information about the penetration depth of light into the water and about the spectral characteristics of the water at different water depths. Above- and in-water radiometric measurements were taken mainly in sunny conditions without cloud overcast. At some stations radiometric measurements were taking in overcast situation. To normalize in-water irradiance measurements, continuous above water irradiance measurements were taken throughout the in-water measuring period. The calibration of TRIOS Ramses sensors was done at TRIOS laboratory. Additional dark current measurements were done during the expedition. One sensor on the frame (Figure. 4.1-15) was equipped with a pressure and inclination sensor for a better quality control of the measurements. Intercalibration measurements of both irradiance

sensors as well as the irradiance sensor installed on the handheld 3-radiometer were taken in sunny conditions.

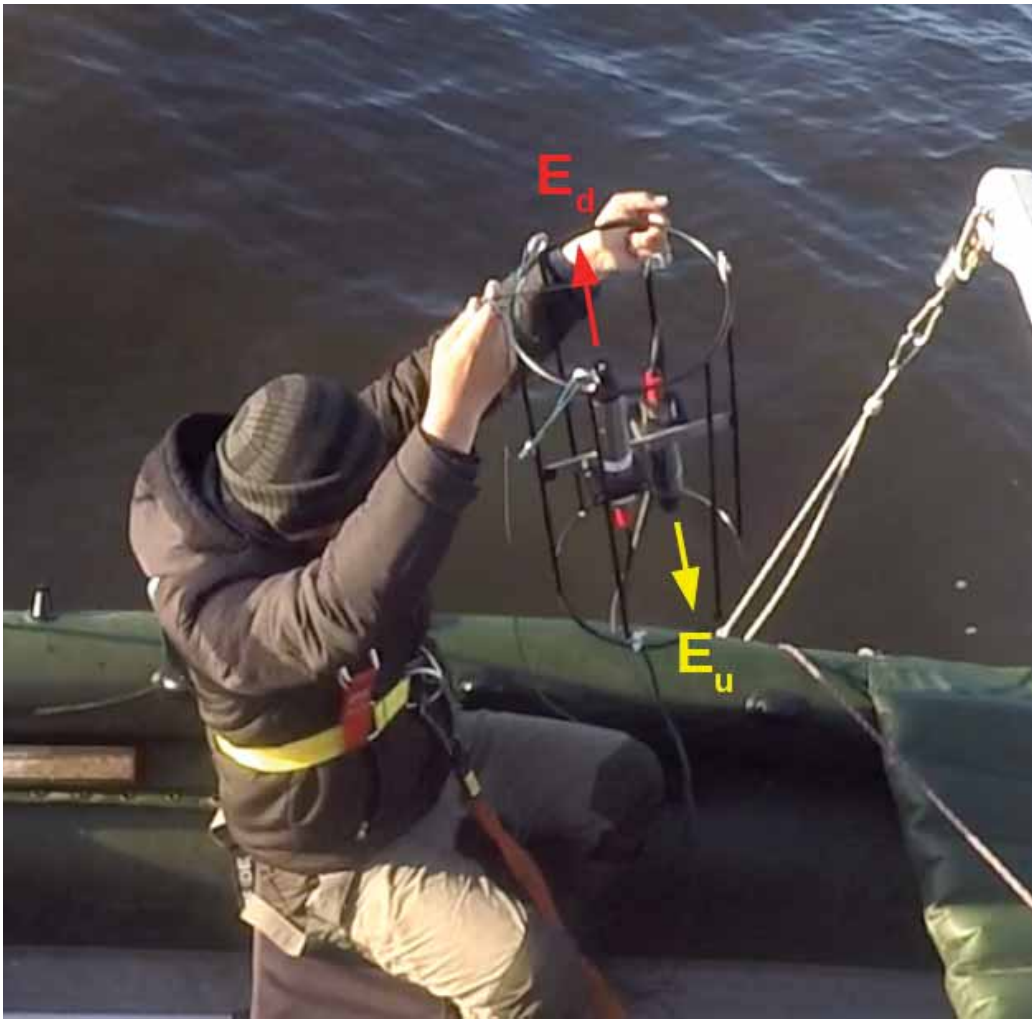

Figure 4.1-15: *Metal frame with two TRIOS Ramses sensor for Irradiance (uplooking sensor for downwelling Irradiance Ed and downlooking sensor for upward irradiance Eu)*

Microtops measurements

Atmospheric parameters such as aerosol optical thickness, direct solar irradiance, and water vapor column were obtained with a Microtops II Sunphotometer. The instrument has 5 spectral bands with centre wavelengths at 380, 440, 500, 675, 870 nm. These measurements are made for additional information for atmospheric correction of satellite images.

Water chemistry

Water column conductivity and temperature were determined with a Sontek CastAway CTD sensor, which measured electrical conductivity with a 6-electrode flow through cell, temperature with a thermistor and water pressure. Locations were automatically saved using onboard GPS, ideally prior to and following each cast.

Water samples were collected for biogeochemical constituents of the water such as suspended particulate matter (SPM), chlorophyll-a (chl-a), coloured dissolved organic matter (cDOM) and dissolved organic carbon (DOC). Furthermore, water samples for stable isotopes, pH, cations and anions were collected. At the majority of stations, only surface water was collected directly into the sampling bottle. At some stations with a higher water depth, also deep water was collected with

an UWITEC^{TM} water sampler. Water samples for SPM (0.5 l) were filtered through pre-rinsed, and pre-weighed 47 mm diameter Whatman GF/F filters with a pore size of 0.7 μm. The filters were dried (50 °C) and the filter weights will be determined at the OSL in St. Petersburg.
For chlorophyll-a, 0.5 l water was filtered through 0.7 μm Whatman GF/F. Further analysis will be done at the OSL in St. Petersburg. The pigments will be extracted from the concentrated algal sample in an aqueous solution of acetone. The chlorophyll-a concentration will be determined spectrophotometrically with a fluorometer TD Trilogy and a spectrophotometer SPECORD 200 by measuring the absorbance (optical density, OD) of the extract at various wavelengths. The resulting absorbance measurements are then applied to a standard equation.
Water for cDOM (0.2 l) was filtered through 0.22 μm GSWP filters. The filter was pre-washed with approx.20 ml Milli-Q water and approx. 20 ml of the seawater sample. After washing the filter, 250 ml of seawater was filtered. 50 ml of the filtrate was used to rinse the storage bottles. The rest of the filtrate (100 ml) was filled into two storage bottles and stored in a dark and cold place. The CDOM analysis will be carried out with a SPECORD 200 spectrophotometer at the OSL in St. Petersburg.
Water samples for DOC were filtered through a pre-rinsed disposable GF/F syringe prefilter 0.7 μm pore size. 20 ml filtrate was filled into a glass vial and 25 ul of 30 % HCl was added for conservation.
At most surface water sampling stations, samples were collected for the analyses of stable isotopes of water (30 ml), major cations/total elements (15 ml, filtered through 0.45 μm pore size cellulose acetate filters and conserved with 65 % HNO_3), major anions (8 ml, filtered through 0.45 μm pore size cellulose acetate filters) and pH and electrical conductivity were measured within 24 hours using a WTW field probe. All samples were kept cool in the field and during transport from the field. Water level was monitored at irregular intervals using staff gauges graduated at 2 cm intervals inserted into the sediment. Four staff gauges spread out over a distance of about 50 m were required to cover the range of water levels between minimum and maximum water levels observed during the field camp. Measurements were made by observing the height of the water on one of the staff gauges. Simultaneous measurements were made when water covered more than one staff gauge to provide correspondence between gauges.
Water column electrical conductivity, salinity and temperature were measured using a Sontek CastAway CTD with built-in GPS. The CTD was placed in recording mode, held beneath the water surface for approx. 10 seconds to allow temperature equilibration, then allowed to fall through the water column in a controlled manner, and then retrieved. Data were recorded during both downward and upward travel.
Sediments were sampled for dating at AWI's MICADAS $\delta^{14}C$ dating laboratory. This included sediment samples, thawed and frozen, from the eroding coastal bluff at Cape Mamontovy Klyk, and offshore surface sediments. Samples were collected using an ice hammer and spoon, collected in glass jars that had been previously purified at temperatures sufficiently high to burn off carbon compounds and covered with foil.
Coastline position was measured relative to terrestrial benchmarks at Cape Mamontovy Khayata on the Bykovsky Peninsula (approx. 71.7837°N, 129.4131°E) and on Muostakh Island, south of the Peninsula (approx. 71.6116°N, 129.9449°E). For these purposes the distance between the benchmark and edge of the undisturbed tundra at the upper edge of the coastal bluff were measured to the nearest centimetre using a measuring tape. Direction was chosen based on the shortest distance between the benchmark and the bluff edge. These measurements continue long-term series of point measurements of coastline position (e.g. Overduin et al., 2015).

Results

Meteorological observations

Air temperatures during the field campaign varied between 0 and 19 °C. Precipitation fell as rain and reached up to a recorded 7 mm/d, although undercatch due to high wind speeds probably skewed these results towards lower than actual values (Figure. 4.1-16). Winds of up to 14 m/s blew mostly from the northwest and northeast and wind direction was highly variable, changing at times more than once a day (Figure. 4.1-17,4.1-18). Air pressure rose and fell repeatedly over a period of approx. 3 - 5 days, with a generally decreasing trend from over 1020 hPa at the beginning of the field season on July 13, to less than 1000 hPa by August 4th. These variations were roughly paralleled by changes in water level in Uomullyakh-Kyuel Lagoon (Figure. 4.1-18). Changes in water level were sometimes very rapid (Figure 4.1-19), for example a variation of half a meter in less than 12 hours on July 23-24. The result of these changes included rapidly changing bathymetry in the lagoon and high rates of discharge or inflow at the two open channels between the lagoon and Tiksi Bay.

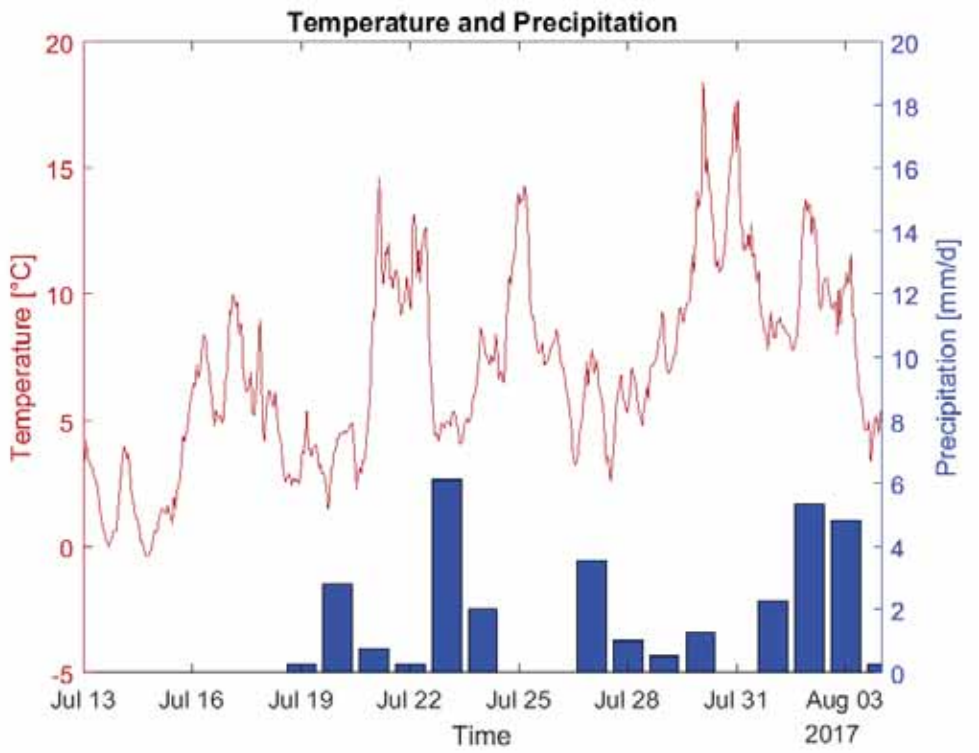

Figure 4.1-16: *Air temperature and precipitation per day during the expedition*

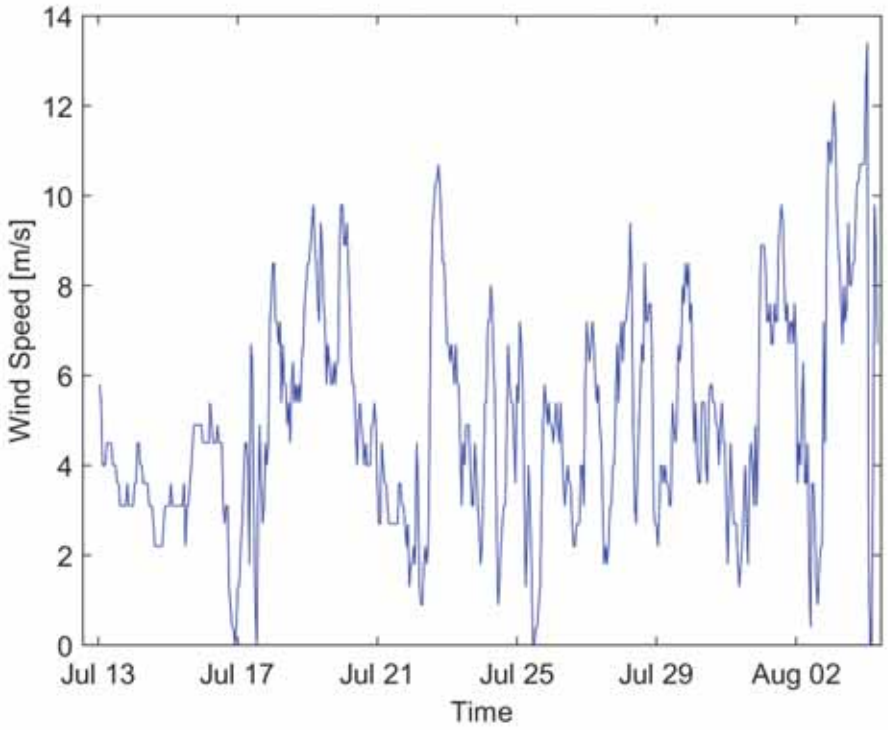

Figure 4.1-17: *Hourly wind speed*

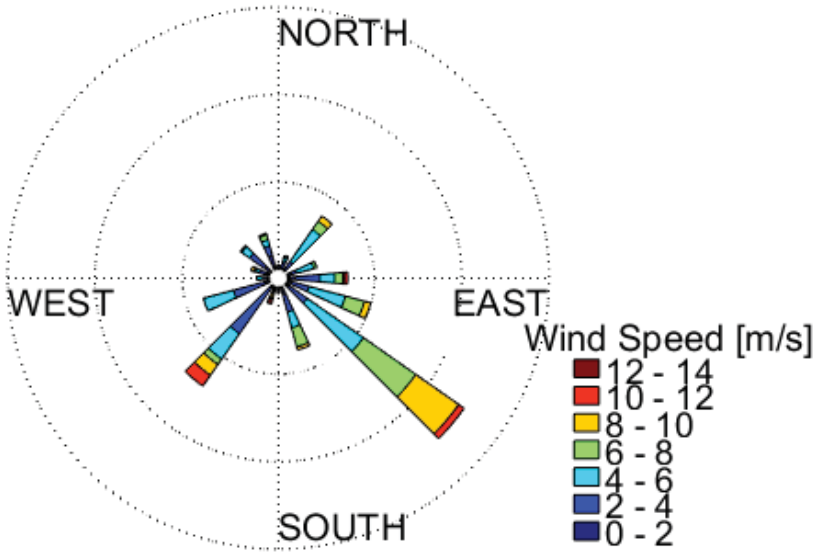

Figure 4.1-18: *Wind rose*

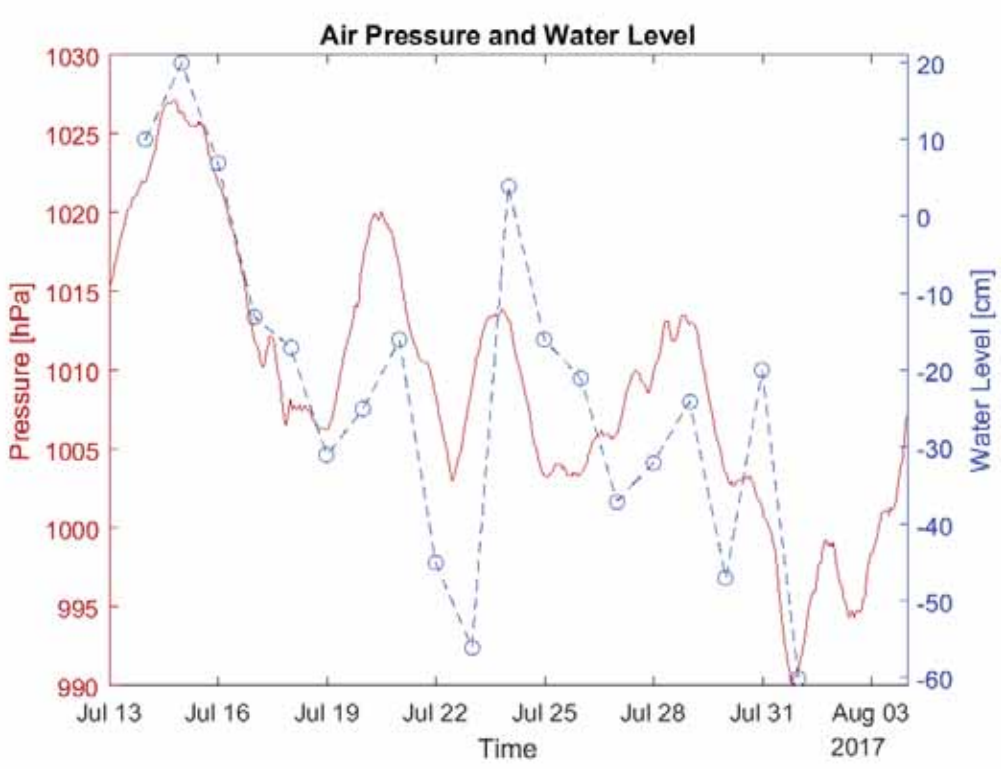

Figure 4.1-19: *Air pressure and water level during the expedition*

4.2 Bibliography

Annan A.P. (2004): Ground penetrating radar principles, procedures and applications.

Angelopoulos M.C., Pollard W.H., Couture N.J. (2013): The application of CCR and GPR to characterize ground ice conditions at Parsons Lake, Northwest Territories. Cold Regions Science and Technology 85, pp. 22-33.

Kneisel C., Hauck C., Fortier R., Moorman B. (2008): Advances in geophysical methods for permafrost investigations. Permafrost and Periglacial Processes 19 (2), pp. 157-178.

Moorman B.J., Robinson S.D., Burgess M.M. (2003): Imaging periglacial conditions with ground-penetrating radar. Permafrost and Periglacial Processes 14 (4), pp. 319-329.

Overduin P.P., Westermann S., Yoshikawa K., Haberlau T., Romanovsky V., Wetterich, S. (2012): Geoelectric observations of the degradation of nearshore submarine permafrost at Barrow (Alaskan Beaufort Sea). Journal of Geophysical Research 117. F02004, doi:10.1029/2011JF002088.

Overduin P.P., Haberland C., Ryberg T., Kneier F., Jacobi T., Grigoriev M.N., Ohrnberger M. (2015): Submarine permafrost depth from ambient seismic noise: Geophysical Research Letters. doi:10.1002/2015GL065409.

Overduin P.P., Blender F., Bolshiyanov D.Y., Grigoriev M.N., Morgenstern A., Meyer H. (2017): Russian-German Cooperation: Expeditions to Siberia in 2016, Berichte zur Polar- und Meeresforschung 709, pp. 295.

Romanovskii N.N., Hubberten H.W., Gavrilov A.V., Tumskoy V.E., Kholodov A.L. (2004): Permafrost of the east Siberian Arctic shelf and coastal lowlands. Quaternary Science Reviews 23 (11), pp. 1359-1369.